UCRL-10814

University of California

Ernest O. Lawrence Radiation Laboratory

THE FORMATION OF DIAMOND-SHAPED PRISMATIC LOOPS IN QUENCHED FCC METALS

TWO-WEEK LOAN COPY

This is a Library Circulating Copy which may be borrowed for two weeks. For a personal retention copy, call Tech. Info. Division, Ext. 5545

DISCLAIMER

This document was prepared as an account of work sponsored by the United States Government. While this document is believed to contain correct information, neither the United States Government nor any agency thereof, nor the Regents of the University of California, nor any of their employees, makes any warranty, express or implied, or assumes any legal responsibility for the accuracy, completeness, or usefulness of any information, apparatus, product, or process disclosed, or represents that its use would not infringe privately owned rights. Reference herein to any specific commercial product, process, or service by its trade name, trademark, manufacturer, or otherwise, does not necessarily constitute or imply its endorsement, recommendation, or favoring by the United States Government or any agency thereof, or the Regents of the University of California. The views and opinions of authors expressed herein do not necessarily state or reflect those of the United States Government or any agency thereof or the Regents of the University of California.

Submitted to J. Applied Physics

UCRL-10814

UNIVERSITY OF CALIFORNIA
Lawrence Radiation Laboratory
Berkeley, California

Contract No. W-7405-eng-48

THE FORMATION OF DIAMOND-SHAPED PRISMATIC LOOPS IN QUENCHED FCC METALS

Alf Eikum and G. Thomas

May 1963

THE FORMATION OF DIAMOND-SHAPED PRISMATIC LOOPS IN QUENCHED FCC METALS

Alf Eikum and G. Thomas

Department of Mineral Technology and
Inorganic Materials Research Division
Lawrence Radiation Laboratory
University of California
Berkeley

Abstract

The concept of dissociated prismatic dislocation loops is proposed to explain the formation of diamond-shaped loops observed in several metals after quench aging. The dissociated prismatic loop is composed of parallel segments on {111} planes having $\frac{a}{6}\langle 112\rangle$ Burgers vectors. It is shown that diamond-shaped loops form from either a triangular or hexagonal Frank loop, and once formed can rotate on the glide cylinder to any orientation between and including {111} and {110}.

Climb kinetics are qualitatively discussed in terms of the equilibrium separation of partials. The separation is approximately equal to the core radius ($2|\vec{b}|$) in Al, but is large enough in Cu ($\sim 12|\vec{b}|$) to be experimentally detected. These considerations may explain why large loops are not often observed in metals other than aluminum.

I. INTRODUCTION

The vacancy supersaturation which can be retained in metals by quenching may be subsequently eliminated by the formation of a variety of dislocation configurations. Prismatic dislocation loops are the most commonly observed defect in pure FCC metals which have been quenched from near the melting point. However, as a result of numerous investigations, (e.g., see reviews in references 1, 2) it has been found that a high density of loops is only observed in aluminum, whereas, in copper, silver and nickel, prismatic loops are normally associated with dislocation tangles. These results suggest that loops can be nucleated homogeneously and heterogeneously. Quenched gold, which represents a lower limit of stacking fault energy for pure metals, contains stacking fault tetrahedra.[3,4]

The mechanism of loop nucleation and the processes by which ultimately observed structures are formed are still not well understood. Idealy, one would hope to understand differences in quench aging behavior for various metals in terms of a few pertinent parameters. For example, in cases where impurity concentration and stress effects have been minimized the type of defect appears to be strongly dependent on stacking fault energy, vacancy supersaturation and vacancy clustering rate. The latter two parameters can in turn be described by vacancy formation energy (E_f) and vacancy migration energy (E_m). Secondly, the effect of impurities, which change the supersaturation when there is a vacancy-impurity interaction,[2,4-8] and the effect of applied stress, both mechanical and thermal, on the quench aging processes should be amenable to systematic study. These latter cases will not be discussed here.

The clustering of vacancies and subsequent collapse into prismatic loops was theoretically discussed by Kuhlmann-Wilsdorf[9] prior to the first

direct observations of loops in aluminum made by Hirsch et al.[10] Although her predictions that the stacking fault energy determines whether perfect or imperfect loops are formed have been qualitatively verified, large Frank loops have been observed recently in very pure aluminum.[4,11] There is little direct information regarding the initial stages of vacancy clustering although spherical clusters have been detected as the initial quench aging defect in copper.[12,13]

It appears from the work of Jackson[14] that both spherical and planar clusters are possible as an initial defect, with the choice being primarily a function of the vacancy supersaturation. However, spherical clusters seem to account for the majority of experimental observations. Collapse of vacancy clusters directly into faulted tetrahedra and subsequent growth by vacancy precipitation have recently been discussed by Thomas and Washburn[2] and de Jong and Koehler.[15] The tetrahedron can be a stable configuration (e.g., in gold) or can degenerate into a triangular Frank loop by nucleation of a Shockley partial dislocation. Nucleation of a Shockley partial can occur spontaneously if the energy difference between tetrahedron and Frank loop is sufficiently large, or the reaction can occur as a result of stresses introduced during quenching. The quench aging sequence, vacancy cluster→faulted tetrahedron→Frank loop→perfect loop, appears more reasonable than vacancy cluster→Frank loop→faulted tetrahedron or glissile loop.[2] In either case, a triangular Frank loop is formed at some stage during aging.

In metals such as Al and Cu, it is observed that perfect diamond-shaped loops are the final and stable configuration. It is the object of this paper to discuss the geometry of the transformation from triangular Frank loops to diamond-shaped loops. This particular case can be discussed in terms of a <u>partial prismatic dislocation loop</u>. That is, the dislocation

loop does not have, strictly speaking, a $\frac{a}{2}\langle 110\rangle$ Burgers vector but is composed of two parallel loops having $\frac{a}{6}\langle 112\rangle$ Burgers vectors. In aluminum the separation distance between two partials is of the order of the core radius but it can be appreciable for gold and copper. It will also be shown that growth of a hexagonal $\frac{a}{2}\langle 110\rangle$ loop yields a final orientation exactly equivalent to that formed by growth of a triangular loop.

II. PARTIAL PRISMATIC LOOPS

Consider the triangular loop in Fig. 1 to have formed from a symmetrical cluster, e.g., a tetrahedron. The Frank loop, $\vec{b} = \frac{a}{3}[111]$ can then be transformed to a perfect loop by nucleation of a Shockley partial[9,16] which can grow by vacancy absorption, or the Frank loop can remain untransformed and itself grow under an adequate supersaturation.

Case A: $\frac{a}{2}\langle 110\rangle$ Prismatic Climb

The growth sequence is illustrated in Fig. 1. Figure 1a represents a triangular perfect loop on $(\bar{1}\bar{1}\bar{1})$. The line segments BC and CA are on $(11\bar{1})$ and $(1\bar{1}1)$ respectively, and, as its Burgers vector $\frac{a}{2}[011]$ is common to $(11\bar{1})$ and $(1\bar{1}1)$, these two segments can dissociate as follows:

$$(11\bar{1}),\ \frac{a}{2}[011] \rightarrow \frac{a}{6}[112] + \frac{a}{6}[\bar{1}21] \qquad (1a)$$

$$(1\bar{1}1),\ \frac{a}{2}[011] \rightarrow \frac{a}{6}[121] + \frac{a}{6}[\bar{1}12] \qquad (1b)$$

A triangular loop with two segments dissociated is shown in Fig. 1b. Thompson's notation[17] is used in some cases for ease of representation and the previous reactions are equivalent to

$$DC \rightarrow D\alpha + \alpha C \quad \text{on } \alpha \qquad (1c)$$

$$DC \rightarrow D\beta + \beta C \quad \text{on } \beta \qquad (1d)$$

The segment AB is pure edge on (100) and, remaining perfect, can more readily climb than BC or CA. Climb of AB in the [100] direction will occur

concurrently with glide along the [011] direction, yielding a final loop shape which is shown in Fig. 1c. This diamond-shaped loop lies entirely in (111) having a major axis parallel to $[2\bar{1}\bar{1}]$ and a minor axis parallel to $[01\bar{1}]$.

It should be noted that the illustration is greatly over simplified; for example, the line segments are expected to be jogged rather than straight as shown. Also, the nodes can range from being extended, as shown, to the opposite extreme of being contracted. These details should not change the general conclusions with respect to the equilibrium shape.

The equilibrium separation of partials was estimated for several metals. The variation in separation $\frac{\bar{x}}{|\bar{b}|}$ as a function of $(\frac{G}{\gamma})$ for the indicated values of the stacking fault energy γ is shown in Fig. 2. G is the shear modulus. The separation for aluminum is seen to be of the order of $2|\bar{b}|$, i.e., what one can consider to be the approximate core radius. A tendency for formation of diamond loops in aluminum thus implies a lowering of core energy which may become more important in aluminum alloys. An example of this type of loop found in Al-5.6 at.% Mg alloy is shown in Fig. 3. Also, the helical dislocation in Fig. 3 appears to have a geometry similar to the loops. It was noted in previous work[7] that helical dislocations became angular even when thin foils were aged in the electron microscope heating stage. The relatively high value of $\bar{x}$ for Cu, indicating a reduced rate of climb, may be an important reason why loops in quenched copper are small.[13] This point will be discussed in section III. A rare example of large loops in Cu-2 at.% Ag after quenching from 1000°C and aging 1 hr. at 100°C is shown in Fig. 4a. The truncated hexagonal loop is ~ 1000 Å in diameter, which is larger than the diamond loops found in the same grain (Fig. 4b).

Case B: $\frac{a}{3}$ <111> Prismatic Climb

The prismatic $\frac{a}{3}$ [111] loop (Frank sessile) is pure edge and can readily grow provided the vacancy supersaturation is sufficiently high to overcome both an increase in line energy and an increase in surface energy. That is, $(\text{Force})_{\text{chem.}} > (\text{Force})_{\text{loop}}$, where $F_{\text{chem}} = \frac{kT}{\bar{b}^2} \ln \frac{c}{c_o}$ (Bardeen and Herring[18]), $\frac{c}{c_o}$ is the vacancy supersaturation, $\bar{b}$ the loop Burgers vector, and kT has the usual meaning. The dislocation line tension derived from circular geometry is considered even though we are discussing triangular, hexagonal and diamond-shaped loops. That is, line tension $\{F(r)\}$ readily illustrates the relative stability of loop "apices" and straight segments in the presence of a vacancy supersaturation. The total energy of a circular Frank loop can be estimated to be,[19,20]

$$E(r) = \frac{G\bar{b}^2 r}{2(1-\nu)} \left[\ln \frac{4r}{\bar{b}} - 1\right] + 8\pi^2 r E_c' + \pi r^2 \gamma \qquad (2)$$

where the core radius has been assumed equal to $2|\bar{b}|$, G is the shear modulus, $\bar{b}$ the Burgers vector, ν is Poisson's ratio, and r the loop radius. The core energy is given in terms of the average energy contribution per atom in the core (E_c') per unit length of dislocation and γ is the stacking fault energy.

The change in total energy E(r) with loop radius can now be found by differentiating Eq. (2), or, for a loop with length $2\pi r$ the line tension is

$$F(r) = \frac{G\bar{b}^2}{4\pi(1-\nu)} \frac{1}{r} \left\{\ln \frac{r}{\bar{b}} + K\right\} + \gamma \qquad (3)$$

where $$K = \frac{16\pi^2(1-\nu)}{G\bar{b}^2} \frac{E_c}{10} + 1.4$$

The energy per core atom (E_c') has been replaced by the core energy (E_c) per unit length of line. There are approximately 10 atoms contributing in this core with radius $2|\bar{b}|$. The value of K will be in the range 2.5 -3.0 depending on which value of E_c is used. A lower limit is $\sim \frac{\mu\bar{b}^2}{10}$,[21] giving

$K \simeq 2.5$, or, by assuming the core to be molten, one finds $E_c \sim \frac{\mu b^2}{5}$ and $K \simeq 3.0$. The lower limit estimate seems better for loops growing at low temperature (20-200°C) which is the case of interest here, though there is little difference.

The condition for loop growth is given by,

$$\frac{kT}{b^2} \ln \frac{c}{c_o} > \frac{Gb^2}{4\pi(1-\nu)} \frac{1}{r} \left(\ln \frac{r}{b} + K\right) + \gamma \qquad (4)$$

A triangular loop can climb into two possible orientations as shown in Fig. 5. For a constant volume of precipitated vacancies, the hexagonal defect represents a decrease in total line energy of approximately 18%. Thus, the hexagonal defect is the more stable form. Also, the climb kinetics will vary around the triangular circumference as the radii of curvature at corners is much greater than that at the sides. Corners will climb under a constant vacancy supersaturation at a slower rate than the straight segments, to continuously increase the radius of curvature. Initially, the corners might be expected to act as vacancy sources. The configuration illustrated in Fig. 5a represents a conservation of <110> line segments, as one would expect. If the line energy of a dislocation is lowered by lying along <112> the orientation in Fig. 5b results.

The hexagonal $\frac{a}{3}$ [111] loop will be stable and continue to climb until the size is sufficiently large to nucleate a Shockley partial to convert it to a glissile $\frac{a}{2}$ <110> loop. A local stress may aid this transformation. In the transformation of a Frank to a perfect loop, if the $\frac{a}{3}$ [111] loop has conserved <110> line segments (Fig. 5a), the resulting $\frac{a}{2}$ [011] loop will climb into the equilibrium configuration illustrated in Fig. 6, which is seen to be indistinguishable from that in Fig. 1c, (the case considered for triangular Frank loops).

A hexagonal faulted loop with <112> segments (Fig. 5b) will behave differently from the case just considered. The line segments of the resultant $\frac{a}{2}$ [011] loop cannot dissociate into partials, the glide cylinder including four {113} planes and two {110} planes. Since a transformation from a hexagonal to a diamond loop requires an energy increase estimated to be ~ 13%, the former orientation should be the more stable.

A diamond loop with sides along <110> directions (Case A or B) is free to slip along its glide cylinder and can lower its line energy by so doing. Therefore, the loop can lie at any position between and including (111) and (011) planes. If the loop does slip into the (011) orientation, the major axis becomes [100] with no change in minor axis. The loop will be in pure edge orientation with sides along <112>. On the other hand, the loop can rotate into any position, as discussed recently by Makin and Hudson[22] for loops on {012}.

III. CLIMB KINETICS

The climb kinetics of dissociated $\frac{a}{2}$ <110> prismatic loops are expected to be different from those of perfect loops. The difference should be primarily a function of the separation $\bar{x}$ of the partials around the loop (Fig. 1c) which varies from metal to metal (Fig. 2). The rate of increase of size of loops can be expressed by,

$$\dot{r} = c_j v_j \tag{5}$$

where c_j is the equilibrium concentration of jogs on the loop and v_j the mean velocity of jogs along the loop.[21]

For the case of dissociated loops, the jog energy (E_j) will be a function of the stacking fault energy, but the exact relationship is difficult to determine because it is not certain whether the jog is contracted

or extended.[23,24] A simple approach lies in defining a unit jog such that the total jog energy can be computed as a function of the separation of the partial dislocations

$$c_j \simeq \exp\left\{-w\, E_j/kT\right\} \qquad (6)$$

The parameter w $(= \frac{1}{2}\frac{\bar{x}}{|\bar{b}|})$ has been chosen so that Eq. (6) reduces to that normally used when discussing undissociated dislocations.[21]

One might expect that v_j for jogs on extended dislocations will vary linearly with stacking fault energy, i.e., to move the jog a distance of one b along the dislocation line requires some number n more vacancies than for the same displacement of a simple jog. The expression for jog velocity should then be that given by Friedel,[21] but decreased by the factor w^{-1}. At the present time, attempts are being made to compare calculated climb rates to those observed directly using high temperature electron microscopy.

IV. SUMMARY

The concept of a dissociated prismatic dislocation loop has been proposed to explain the diamond-shaped loops which are observed after the quench aging of several metals. A diamond loop can be formed from the growth of either perfect or imperfect triangular or hexagonal prismatic loops, the two cases being indistinguishable.

It has been shown that the climb kinetics are a sensitive function of the stacking fault energy. This may be an important factor in explaining why the loops observed in copper and other metals are relatively small compared to those found in aluminum.

Acknowledgment

The authors thank the United States Atomic Energy Commission for financial support of this work.

References

1. M. J. Whelan, Electron Microscopy and Strength of Crystals, Eds., G. Thomas and J. Washburn (Interscience Publishers, New York, 1962) p. 3.
2. G. Thomas and J. Washburn (AIME Symposium on Point Defects, Dallas, March 1963) to be published.
3. J. Silcox and P. B. Hirsch, Phil. Mag., 4, 72 (1959).
4. R. M. J. Cotterill and R. L. Segall (Fifth International Congress for Electron Microscopy, Philadelphia, August 1962) p. J-13.
5. G. Thomas, Phil. Mag., 4, 606, 1213 (1959).
6. K. H. Westmacott, R. S. Barnes, D. Hull and R. E. Smallman, Phil. Mag. 6, 829 (1961).
7. A. Eikum and G. Thomas (International Conference on Crystal Lattice Defects, Kyoto Japan, 1962) Japanese J. Phys., in press.
8. J. D. Embury and R. B. Nicholson, Acta. Met., 11, 347 (1963).
9. D. Kuhlmann-Wilsdorf, Phil. Mag., 3, 125 (1958).
10. P. B. Hirsch, J. Silcox, R. E. Smallman and K. H. Westmacott, Phil. Mag. 3, 897 (1958).
11. S. Yoshida, M. Kiritani and Y. Shimomura, J. Phys. Soc. Japan, 18, 175 (1963).
12. J. Galligan and J. Washburn, UCRL Report 10606 Rev. (1963).
13. K. Chik, A. Seeger and M. Ruhle (Fifth International Congress for Electron Microscopy, Philadelphia, August 1962) p. J-11.
14. K. A. Jackson, Phil. Mag., 7, 1117 (1962).
15. M. de Jong and J. S. Koehler, Phys. Rev., 129, 49 (1963).
16. G. Saada, Acta Met., 10, 551, 985 (1962).
17. N. Thompson, Proc. Phys. Soc., 66, 481 (1953).
18. J. Bardeen and C. Herring, Atom Movements (ASM 1951) p. 87.
19. H. Franz and E. Kroener, Z. Metallk., 46, 639 (1959).

20. G. Schoeck and W. A. Tiller, Phil. Mag., 5, 43 (1960).

21. J. Friedel, Les Dislocations (Gauthier-Villars, Paris, 1956).

22. M. J. Makin and B. Hudson, Phil. Mag., 8, 447 (1963).

23. A. Seeger, Report on the Bristol Conference on Defects in Crystalline Solids (The Physical Society, London-1955) p. 391.

24. P. B. Hirsch, Phil. Mag., 7, 67 (1962).

Figure Captions

Fig. 1 Climb geometry of the $\frac{a}{2}$ [011] prismatic loop; (a) perfect triangular loop, (b) after dissociation of two segments into $\frac{a}{6}$ <112> orientation, (c) equilibrium diamond shape.

Fig. 2 Calculated equilibrium separation between partial dislocations as a function of $(\frac{G}{\gamma})$ for the loop orientation considered in Fig. 1.

Fig. 3 Diamond-shaped prismatic loops in Al-5.6 at.% Mg quenched from 520°C and aged 94 hr. at 100°C. The most probable plane of the loop is (111) or $(\bar{1}\bar{1}1)$.

Fig. 4 Loops found in Cu-2 at.% Ag quenched from 1000°C and aged 1 hr. at 100°C; (a) large truncated Frank loop, (b) diamond-shaped loops.

Fig. 5 Climb geometry of the triangular $\frac{a}{3}$ [111] prismatic loop into hexagonal orientation; (a) with <110> line segments conserved, (b) with <112> line segments formed.

Fig. 6 Climb geometry of the hexagonal $\frac{a}{2}$ [011] prismatic loop into the equilibrium diamond orientation.

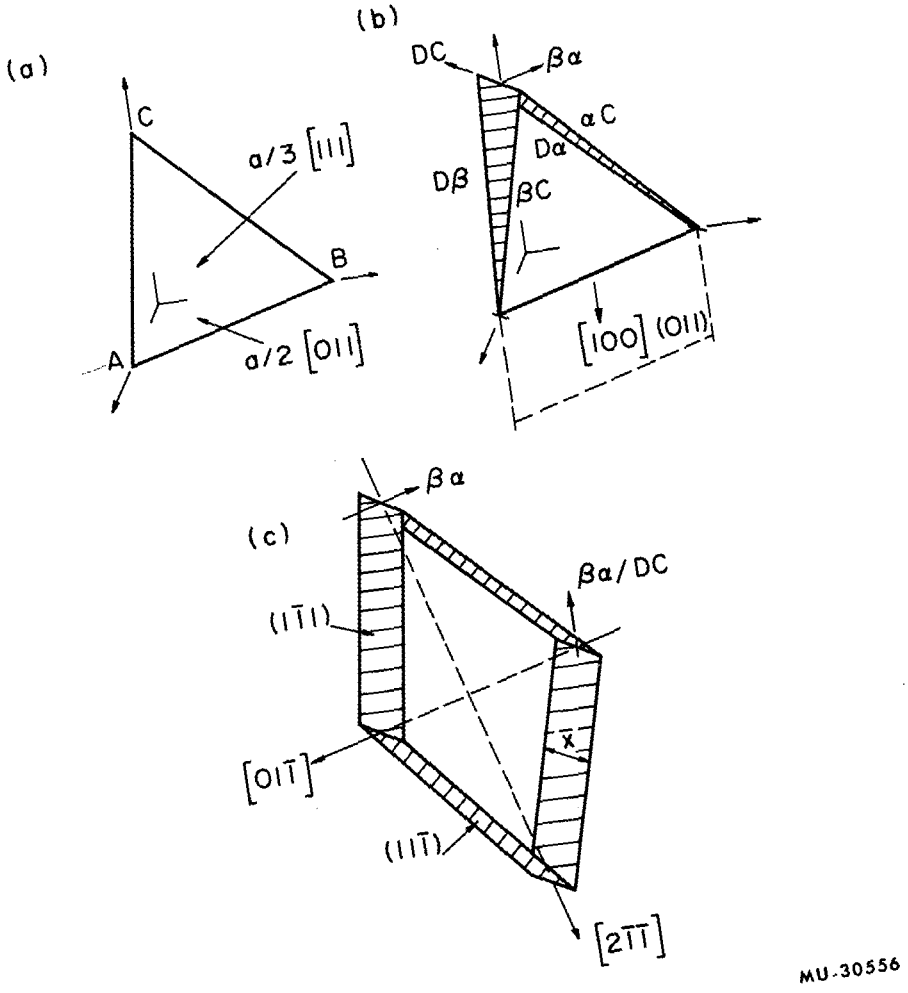
(a)
C
a/3 [111]
B
A
a/2 [011]
(b)
DC
βa
αC
Dα
Dβ
βC
[100] (011)
(c)
βa
βa/DC
(1$\bar{1}$1)
[01$\bar{1}$]
x
(11$\bar{1}$)
[2$\bar{1}\bar{1}$]
MU-30556

Fig. 1.

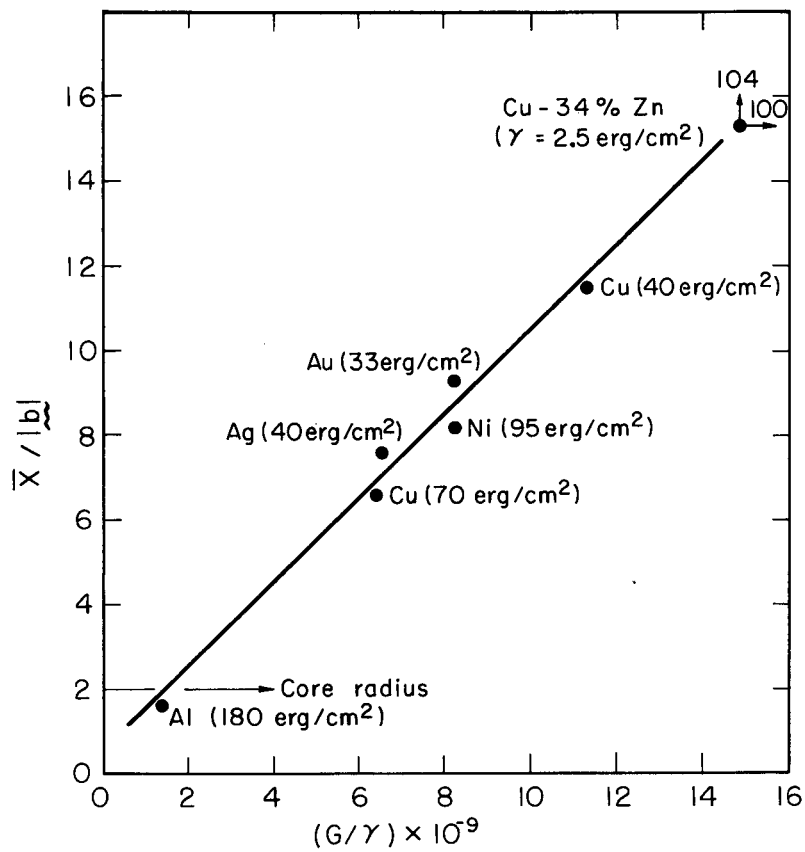

MU-30557

Fig. 2.

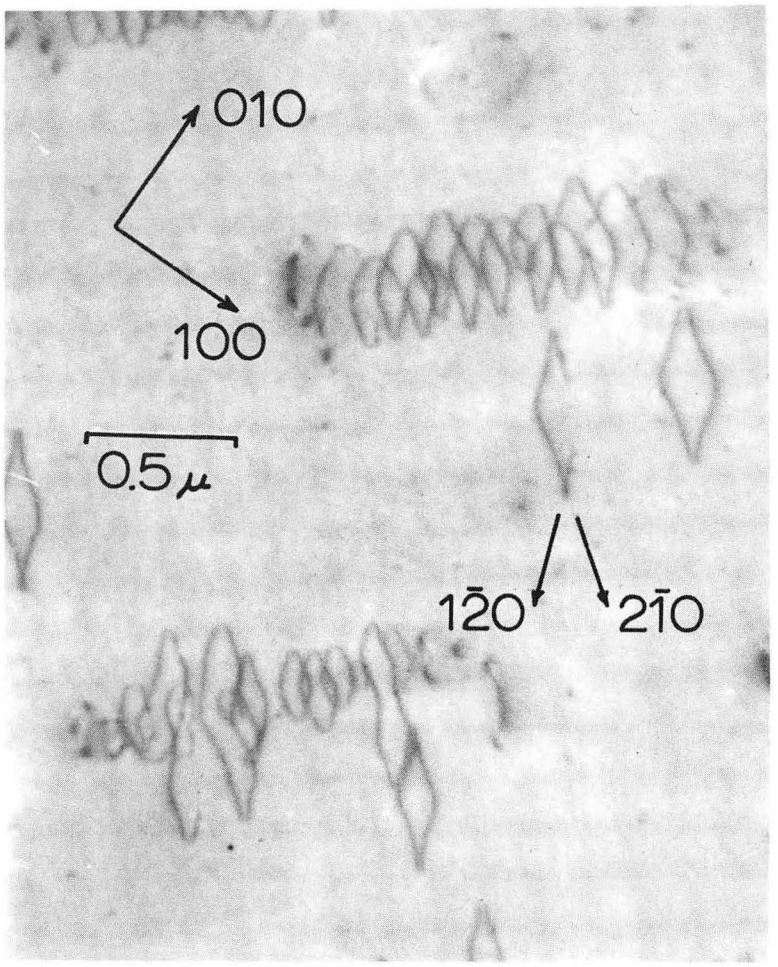

ZN-3629

Fig. 3.

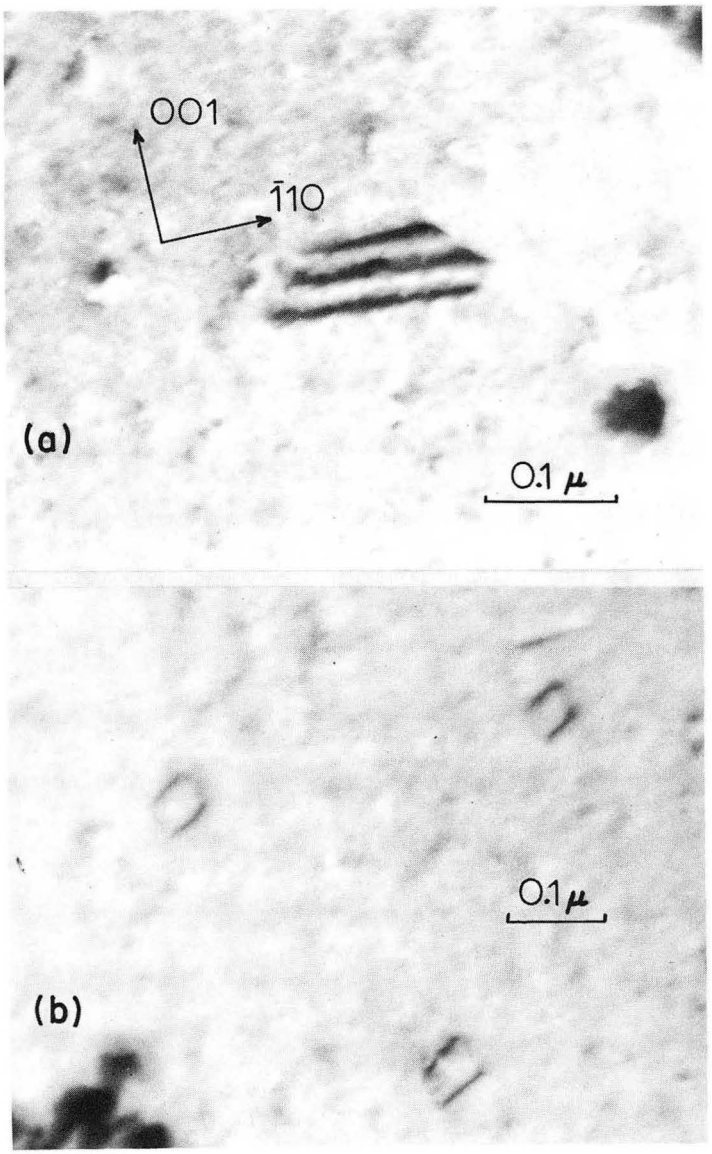

ZN-3789

Fig. 4.

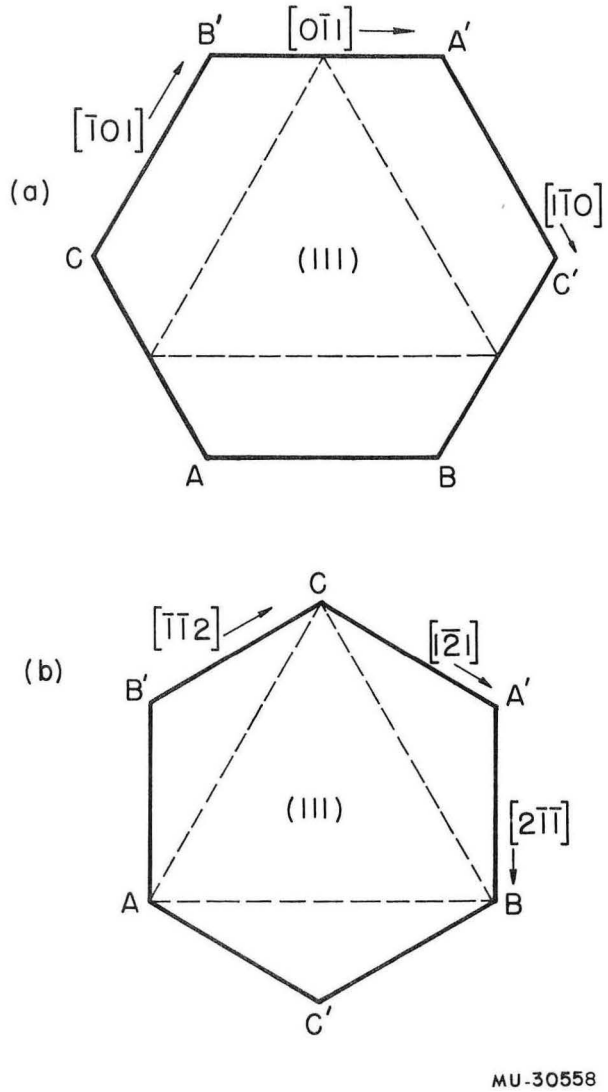
(a)
B′
[0$\bar{1}$1]
A′
[$\bar{1}$01]
[1$\bar{1}$0]
C
(111)
C′
A
B
(b)
C
[$\bar{1}\bar{1}$2]
[1$\bar{2}$1]
B′
A′
(111)
[2$\bar{1}\bar{1}$]
A
B
C′
MU-30558

Fig. 5.

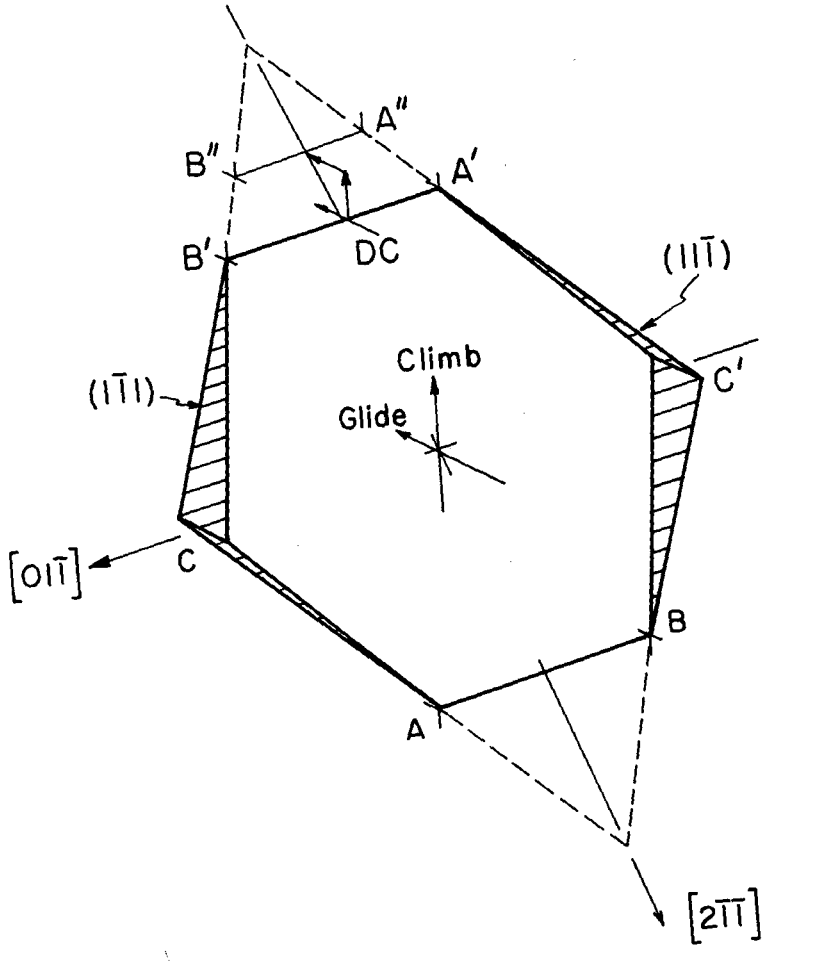
A''
B''
A'
B'
DC
(11$\bar{1}$)
Climb
C'
(1$\bar{1}$1)
Glide
[01$\bar{1}$]
C
B
A
[2$\bar{1}\bar{1}$]
MU-30559

Fig. 6.

This report was prepared as an account of Government sponsored work. Neither the United States, nor the Commission, nor any person acting on behalf of the Commission:

A. Makes any warranty or representation, expressed or implied, with respect to the accuracy, completeness, or usefulness of the information contained in this report, or that the use of any information, apparatus, method, or process disclosed in this report may not infringe privately owned rights; or

B. Assumes any liabilities with respect to the use of, or for damages resulting from the use of any information, apparatus, method, or process disclosed in this report.

As used in the above, "person acting on behalf of the Commission" includes any employee or contractor of the Commission, or employee of such contractor, to the extent that such employee or contractor of the Commission, or employee of such contractor prepares, disseminates, or provides access to, any information pursuant to his employment or contract with the Commission, or his employment with such contractor.